Chapter 6
Spatial Spread with Allee Effect

Abstract Many species exhibit an Allee effect, where population growth rates are highest at intermediate rather than low density, and small populations may even decline. Determining the spread rates of these species turns out to be much more difficult than the theory in the preceding chapter, where there was no Allee effect. Mathematically, this difficulty arises since—just as in the case of steady states—we cannot expect the linearization at zero to give useful information about the behavior of solutions for larger density, and hence we cannot expect the linearization-based spread formulas from the previous chapter to hold. One of the most interesting biological results here is that with the Allee effect, a population may spread or retreat. Hence, eradication of an invading pest species seems possible if management measures could turn an invasion into a retreat. We begin this chapter with a caricature model for which all relevant quantities can be explicitly calculated. Then we present a general condition for whether a population will spread or retreat. Finally, we present a theorem about the existence of traveling waves and the uniqueness of their speed.

6.1 Allee Effects and Biological Invasions

Allee effects (see Sect. 2.2) are ubiquitous in nature, and some are particularly relevant for biological invasions (Taylor and Hastings 2005; Lewis et al. 2016). For example, healthy pine trees produce and exude resin to defend themselves against harmful insects, such as the mountain pine beetle (*Dendroctonus ponderosae* Hopkins). As long as only a few beetles attack a tree, they will die in the resin. When a large number of beetles attack a tree, the resin is insufficient to kill all of them. The tree succumbs and the beetles can reproduce (Powell and Bentz 2014). This is a classical setup for an Allee effect; see also Sect. 12.6.

In the presence of an Allee effect, mathematical analysis becomes more difficult. We already know from the nonspatial model in (2.22) and the steady-state analysis in Sect. 4.5 that the linearization at zero may not provide information about the existence of a positive steady state and that the eventual state of the population may depend on the initial condition. Similarly, in the question of invasions, none of the

F. Lutscher, *Integrodifference Equations in Spatial Ecology*, Interdisciplinary Applied Mathematics 49, https://doi.org/10.1007/978-3-030-29294-2_6

explicit calculations for spread with linear equations from the previous chapter carry over to the case with Allee effect, since the phenomenon is inherently nonlinear.

Throughout this section, we consider a strong Allee effect with a monotone growth function. As always, we can scale steady states to be $F(0) = 0$, $F(1) = 1$, as in (2.22). With a strong Allee effect, there is an *Allee threshold* $N_a \in (0, 1)$ with the property (see Fig. 2.2)

(A1) $F(N) < N$ for $N \in (0, N_a)$ and $F(N) > N$ for $N \in (N_a, 1)$.

For a piecewise-constant caricature Allee function, we can explicitly calculate conditions for spread as well as the corresponding asymptotic speeds (Kot et al. 1996). In Sect. 6.3, we present a simple criterion for the direction of the traveling wave (Wang et al. 2002). The last section is devoted to the more abstract theory of the existence of traveling waves (Lui 1983).

6.2 A Caricature Allee Function

For an analytically tractable example, we choose the piecewise-constant growth function (Kot et al. 1996)

$$F(N) = \begin{cases} 0, & N < N_a \,, \\ 1, & N \geq N_a \,, \end{cases} \tag{6.1}$$

with Allee threshold $N_a \in (0, 1)$ and carrying capacity equal to unity. The population density after the growth phase is either one or zero. As in the previous chapter, we consider a homogeneous landscape and a symmetric dispersal kernel of the form $K(x - y)$.

Because of the Allee effect, we expect the initial spatial extent of a population to determine whether the population will persist and spread or decline and retreat. We assume that the initial population exceeds the Allee threshold exactly on some bounded interval and calculate subsequent densities. Since the landscape is homogeneous and the growth function is binary, we may choose $N_0(x) = \chi_{[-x_0,x_0]}(x)$, the characteristic function of that interval, i.e., $N_0(x) = 1$ if $x \in [-x_0, x_0]$ and $N_0(x) = 0$ otherwise. Then $F(N_0) = N_0$. The density in the next generation is

$$N_1(x) = \int_{-\infty}^{\infty} K(x - y)\chi_{[-x_0,x_0]}(y)\mathrm{d}y = \int_{-x_0}^{x_0} K(x - y)\mathrm{d}y = \int_{x-x_0}^{x+x_0} K(y)\mathrm{d}y \,. \tag{6.2}$$

By symmetry, if $N_1(x) \geq N_a$ for some x, then $N_1(x) \geq N_a$ on some interval $[-x_1, x_1]$, where x_1 satisfies the implicit equation

$$\int_{x_1-x_0}^{x_1+x_0} K(y)\mathrm{d}y = N_a \,. \tag{6.3}$$

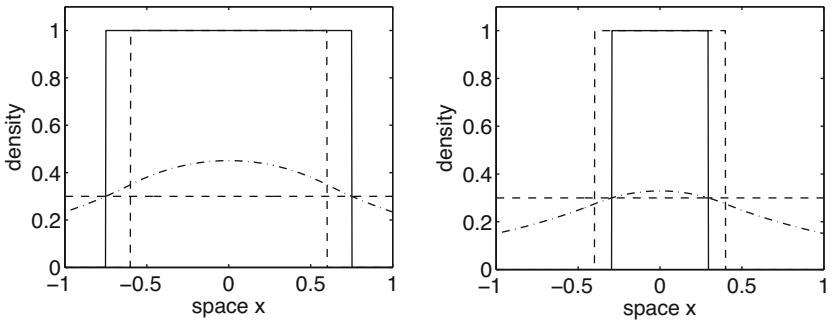

Fig. 6.1 Expansion (left) and retraction (right) with the caricature Allee function in (6.1). The dashed line is the density before dispersal, the dash-dot line is the profile after dispersal, and the solid line represents the density after applying the growth function. The horizontal dashed line indicates the Allee threshold of 0.3. We used the Laplace kernel with dispersal distance one.

After the subsequent growth phase, the population density will be $F(N_1(x)) = \chi_{[-x_1,x_1]}(x)$. Inductively, we obtain the extent x_{t+1} from x_t by solving

$$\int_{x_{t+1}-x_t}^{x_{t+1}+x_t} K(y)\mathrm{d}y = N_a \ . \tag{6.4}$$

We expect that if the initial spatial extent is small, it will shrink over time ($0 \leq x_{t+1} < x_t$) and the population will die out. If the initial extent is large enough, it will grow over time ($x_{t+1} > x_t$) and the population will spread. These two cases are illustrated in Fig. 6.1. We obtain the critical spatial extent where the population remains constant by setting $x_{t+1} = x_t = x_c$ or

$$\int_0^{2x_c} K(y)\mathrm{d}y = N_a \ . \tag{6.5}$$

Since the kernel is a symmetric probability density, the integral is bounded by 1/2. Hence, we require $N_a < 1/2$; otherwise a population cannot persist or spread.

For the Laplace kernel in (2.27) with parameter a, the integral in (6.4) can be evaluated explicitly, but we have to distinguish two cases. When $x_{t+1} > x_t$, we find

$$\int_{x_{t+1}-x_t}^{x_{t+1}+x_t} K(y)\mathrm{d}y = \mathrm{e}^{-ax_{t+1}} \sinh(ax_t) \ . \tag{6.6}$$

Hence, the spatial extent satisfies the difference equation

$$x_{t+1} = \frac{1}{a} \ln\left(\frac{\sinh(ax_t)}{N_a}\right). \tag{6.7}$$

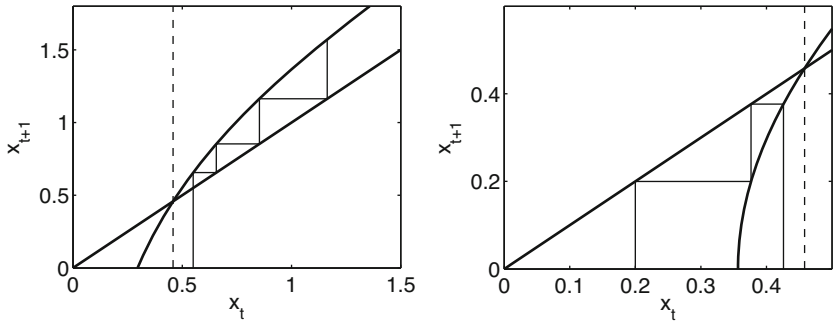

Fig. 6.2 Illustration of the recursions of spatial extent from one generation to the next with Laplace kernel (6.7). The plot on the left illustrates the case $x_{t+1} > x_t \geq x_c$; the plot on the right has the reversed inequalities. The mean dispersal distance is unity, and the Allee threshold is $N_a = 0.3$, so that $x_c \approx 0.4581$ (dashed vertical line).

When $x_{t+1} < x_t$, it is easier to write the backward iteration

$$x_t = \frac{1}{a} \ln\left(\frac{\cosh(a x_{t+1})}{1 - N_a}\right). \tag{6.8}$$

The critical value x_c from (6.5) is given by $2ax_c = -\ln(1 - 2N_a)$. We illustrate the cobweb for both of these iterations in Fig. 6.2 and the critical value as the vertical dashed line.

We can use the same approach to calculate the asymptotic spreading speed for the population. If the population spreads asymptotically with constant speed $c^* > 0$, then $x_{t+1} - x_t \to c^*$ and $x_{t+1} + x_t \to \infty$ as $t \to \infty$. From (6.4), we find c^* implicitly as

$$\int_{c^*}^{\infty} K(z)\mathrm{d}z = N_a \quad \text{or} \quad \int_0^{c^*} K(z)\mathrm{d}z = \frac{1}{2} - N_a \,, \tag{6.9}$$

where we used the symmetry of the kernel again. (Recall also that K is a probability density.)

As before, the necessary condition for spread ($c^* > 0$) is $N_a < 1/2$. For certain kernels, (6.9) can be solved for c^*. For the Gaussian (2.25) and Laplace (2.27) kernel we obtain

$$c^*_{\text{Gauss}} = \sqrt{2\sigma^2}\,\text{erf}^{-1}(1 - 2N_a) \quad \text{and} \quad c^*_{\text{Laplace}} = -\sqrt{\sigma^2/2}\,\ln(2N_a)\,, \tag{6.10}$$

respectively, where $\text{erf}(x)$ is the error function. We plot the speeds for these two kernels in Fig. 6.3 as a function of the variance (left plot). We see that the speed for the Gaussian kernel is lower than for the Laplace kernel when the Allee threshold

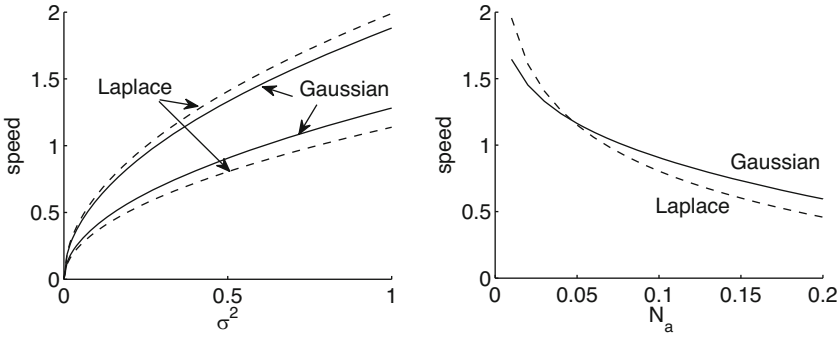

Fig. 6.3 Speeds of spread for the caricature Allee function (6.1) with Gaussian (solid) and Laplace (dashed) kernels. **Left plot:** Speed as a function of variance when $N_a = 0.1$ (lower curves) and $N_a = 0.03$ (upper curves). **Right plot:** The speed of spread as a function of N_a with $\sigma^2 = 0.5$.

is very small, but higher when N_a is large. It turns out that the value N_a^* where the two speeds are equal is independent of the variance. It is implicitly given by

$$2\text{erf}^{-1}(1 - 2N_a^*) = -\ln(2N_a^*) \,. \tag{6.11}$$

We find the critical value numerically as $N_a^* \approx 0.0464$. Figure 6.3 also shows the speed as a function of N_a (right plot).

Several other kernels allow for an explicit calculation of c^* from (6.9). For the double Weibull kernel (see Table 3.1) we calculate

$$c^*_{\text{Weibull}} = \theta \, (-\ln(2N_a))^{1/k} \,. \tag{6.12}$$

For the Cauchy kernel (5.8), we find

$$c^*_{\text{Cauchy}} = \beta \tan\left(\frac{\pi}{2}(1 - 2N_a)\right), \tag{6.13}$$

and for the exponential square root kernel from (5.37), we can use the Lambert W function again (see (5.28)) to find

$$c^*_{\text{ExpRoot}} = \frac{1}{a^2} \, (-W_{-1}(-2N_a/e) - 1)^2 \,. \tag{6.14}$$

We note that both heavy-tailed kernels admit a finite asymptotic spreading speed here because the Allee function ensures that the population occupies only a finite region after the growth phase. In general, however, heavy-tailed kernels can generate accelerating invasions, even with an Allee effect (Wang et al. 2002).

We can use a slight variation of the above reasoning to calculate the speed of a (monotone) traveling wave as well. Clearly, the traveling wave profile, $N^*(x)$, after

the growth phase must have the form of a characteristic function, e.g., $F(N^*(x)) = \chi_{(-\infty,0]}$. Then

$$N^*(x-c) = \int_{-\infty}^{\infty} K(x-y)F(N^*(y))\mathrm{d}y = \int_{x}^{\infty} K(z)\mathrm{d}z = \frac{1}{2} - \int_{0}^{x} K(z)\mathrm{d}z \ . \tag{6.15}$$

After the subsequent growth phase, the profile will be the characteristic function on $(-\infty, c]$, where c is calculated from

$$\frac{1}{2} - \int_{0}^{c} K(z)\mathrm{d}z = N_a \ , \tag{6.16}$$

which is the same as (6.9). When $N_a < 1/2$, then c is positive and the population advances; when $N_a > 1/2$, then c is negative and the population retreats. For $N_a = 1/2$, there is a constant profile with speed zero. This behavior is typical when an Allee effect is present, as we shall see in the next section.

6.3 The Direction of a Traveling Front

We saw that the speed of a traveling front in the IDE with the caricature Allee effect can have any sign; i.e., the front may invade or retreat or remain stationary. Somewhat surprisingly, the direction of the front depends only on the growth function and is independent of the dispersal kernel (as long as it is symmetric). This result by Wang et al. (2002) generalizes the corresponding, well-known result for a reaction-diffusion equation with strong Allee effect (Kot 2001). The proof in the discrete-time case is much more involved. Our exposition follows Wang et al. (2002).

Theorem 6.1 (Wang et al. 2002) *Consider the IDE $N_{t+1}(x) = (K * F(N_t))(x)$ with monotone growth function F and steady states $N = 1$ and $N = 0$. Assume that there is a monotone decreasing traveling front with speed c and profile $N(x)$, connecting the two states; see Fig. 6.4. Furthermore, assume that F and N are real analytic functions, that derivatives of any order of N vanish as $x \to \pm\infty$, and that the derivatives $d^i F(N(x))/dx^i$ are bounded uniformly in i. Then we have the following relation for the sign of the speed of the traveling front:*

$$\mathrm{sign}(c) = \mathrm{sign}\left(\int_0^1 [F(N) - N]\mathrm{d}N\right). \tag{6.17}$$

The integral on the right is the signed area between $F(N)$ and N. The region where $F(N) - N$ is positive (negative) is indicated by a $+$ ($-$) sign in Fig. 6.4. The statement of the theorem does not require a (strong) Allee effect. However, if there is a weak or no Allee effect, then $F(N) > N$ for $0 < N < 1$, and so the integral on the right-hand side will be positive.

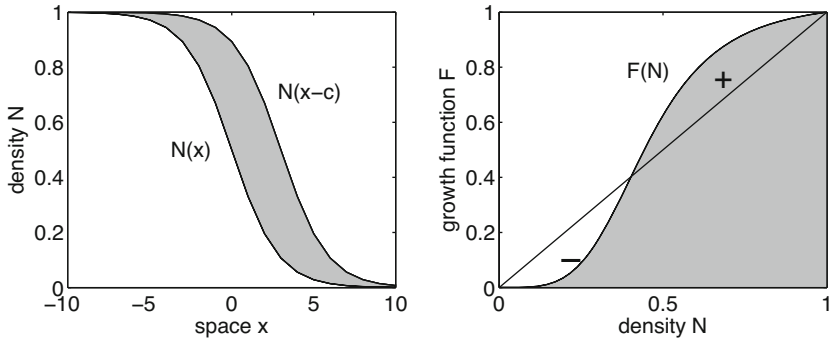

Fig. 6.4 Illustration for Theorem 6.1. **Left plot:** The difference between the traveling front profile in subsequent generations. **Right plot:** Growth function with strong Allee effect and illustration of the integral in (6.17).

Proof Since the front is decreasing, we have $c > 0$ if and only if $N(x) < N(x-c)$ for all x. Since F is monotone increasing and N is monotone decreasing, the derivative

$$\frac{\mathrm{d}F}{\mathrm{d}x} := \frac{\mathrm{d}}{\mathrm{d}x}(F(N(x)) \tag{6.18}$$

is negative. Hence, we find that $c > 0$ if and only if $[N(x) - N(x-c)]\frac{\mathrm{d}F}{\mathrm{d}x} > 0$ for all x. In Lemma 6.1, we show the integral equality

$$\int_{-\infty}^{\infty}[N(x) - N(x-c)]\frac{\mathrm{d}F}{\mathrm{d}x}\mathrm{d}x = \int_{-\infty}^{\infty}[N - F(N)]\frac{\mathrm{d}F}{\mathrm{d}x}\mathrm{d}x\ . \tag{6.19}$$

The transformation of variables $y = F(N(x))$ applied to the integral on the right results in

$$\int_{-\infty}^{\infty}[N - F(N)]\frac{\mathrm{d}F}{\mathrm{d}x}\mathrm{d}x = \int_{0}^{1}[y - F^{-1}(y)]\mathrm{d}y\ . \tag{6.20}$$

The graph of the function $y = F(N)$ partitions the unit square into the gray and white areas in the right plot in Fig. 6.4 so that

$$\int_0^1 F(N)\mathrm{d}N + \int_0^1 F^{-1}(y)\mathrm{d}y = 1\ . \tag{6.21}$$

A similar argument applies to the function $y = N$ so that the expression in (6.20) can be written as

$$\int_0^1 [y - F^{-1}(y)]\mathrm{d}y = 1 - \int_0^1 N\mathrm{d}N - \left(1 - \int_0^1 F(N)\mathrm{d}N\right) = \int_0^1 [F(N) - N]\mathrm{d}N\ . \tag{6.22}$$

Altogether, we find that $c > 0$ if and only if the expression in (6.22) is positive. The same reasoning applies for $c < 0$ and $c = 0$. Hence, the theorem is proved. □

Lemma 6.1 *Under the conditions of Theorem 6.1, integral equality (6.19) holds.*

Proof We need to show the equality

$$\int_{-\infty}^{\infty} N(x-c)\frac{\mathrm{d}F}{\mathrm{d}x}\mathrm{d}x = \int_{-\infty}^{\infty} F(N)\frac{\mathrm{d}F}{\mathrm{d}x}\mathrm{d}x \ . \tag{6.23}$$

In the defining equation for the traveling front,

$$N(x-c) = \int_{-\infty}^{\infty} K(z)F(N(x-z))\mathrm{d}z \ , \tag{6.24}$$

we split $F(N(x-z))$ into its even and odd parts with respect to z, i.e.,

$$F_e(x,z) = \frac{1}{2}[F(N(x-z)+F(N(x+z))], \quad F_o(x,z) = \frac{1}{2}[F(N(x-z)-F(N(x+z))],$$

and obtain

$$N(x-c) = \int_{-\infty}^{\infty} K(z)[F_e(x,z)+F_o(x,z)]\mathrm{d}z = \int_{-\infty}^{\infty} K(z)F_e(x,z)\mathrm{d}z \ . \tag{6.25}$$

The last equality above arises since the integral of the product of an even function and an odd function is zero. Now we multiply the equality in (6.25) by $\mathrm{d}F/\mathrm{d}x$ and integrate. Since the integrand is of one sign, we use Tonelli's theorem to exchange the order of integration and obtain

$$\int_{-\infty}^{\infty} N(x-c)\frac{\mathrm{d}F}{\mathrm{d}x}\mathrm{d}x = \int_{-\infty}^{\infty}\int_{-\infty}^{\infty} K(z)F_e(x,z)\frac{\mathrm{d}F}{\mathrm{d}x}\mathrm{d}x\mathrm{d}z \ . \tag{6.26}$$

Next, we expand F_e in a power series around $z = 0$. Because the function is even, all derivatives of odd order vanish. The derivatives of even order at $z = 0$ are the same as the derivatives of $F(N(x))$. Using the fact that the kernel integrates to unity, we find that the integral above equals

$$\int_{-\infty}^{\infty} F(N(x))\frac{\mathrm{d}F}{\mathrm{d}x}\mathrm{d}x + \int_{-\infty}^{\infty}\int_{-\infty}^{\infty} K(z)\sum_{i=1}^{\infty}\frac{z^{2i}}{(2i)!}\left(\frac{\mathrm{d}^{2i}}{\mathrm{d}x^{2i}}F(N(x))\right)\frac{\mathrm{d}F}{\mathrm{d}x}\mathrm{d}x\mathrm{d}z \ . \tag{6.27}$$

It remains to show that the double integral vanishes. By Levi's theorem, we may interchange summation and the inner integration. Using integration by parts, we verify that each of the inner integrals vanishes as follows. For $i = 1$, we calculate

$$\int_{-\infty}^{\infty} \frac{\mathrm{d}^2}{\mathrm{d}x^2} F(N(x)) \frac{\mathrm{d}F}{\mathrm{d}x} \mathrm{d}x = \frac{1}{2} \left(\frac{\mathrm{d}F}{\mathrm{d}x} \right)^2 \Big|_{-\infty}^{\infty} = 0 \,. \tag{6.28}$$

For $i = 2$, we apply integration by parts twice

$$\begin{aligned} \int_{-\infty}^{\infty} \frac{\mathrm{d}^4}{\mathrm{d}x^4} F(N(x)) \frac{\mathrm{d}F}{\mathrm{d}x} \mathrm{d}x &= \frac{\mathrm{d}^3 F}{\mathrm{d}x^3} \frac{\mathrm{d}F}{\mathrm{d}x} \Big|_{-\infty}^{\infty} - \int_{-\infty}^{\infty} \frac{\mathrm{d}^3}{\mathrm{d}x^3} F(N(x)) \frac{\mathrm{d}^2 F}{\mathrm{d}x^2} \mathrm{d}x \\ &= 0 - \frac{1}{2} \left(\frac{\mathrm{d}^2 F}{\mathrm{d}x^2} \right)^2 \Big|_{-\infty}^{\infty} = 0 \,. \end{aligned} \tag{6.29}$$

Successively, each term in the infinite sum vanishes by repeated application of integration by parts. At this point, we have used the assumption that all derivatives of $N(x)$ vanish as $x \to \pm\infty$ and that all derivatives of F are (uniformly) bounded. □

6.4 General Theory

Explicit calculations for the spreading speed and traveling fronts in an IDE with Allee growth functions are rarely possible. Abstract results about spreading properties and traveling fronts, however, appear simultaneously with those mentioned in the previous chapter when there is no Allee effect (Weinberger 1982; Lui 1983). Clearly, there cannot be a formula analogous to (5.17) for a spreading speed based on the linearization at zero, but that formula can be used to bound the spreading speed even in the case with Allee effect (Lui 1983). Since a population may retreat and not advance, it is also clear that Definition 5.1 of the asymptotic spreading speed cannot apply in the presence of an Allee effect. In particular, the example in Sect. 6.2 shows that a locally introduced population with Allee effect may collapse below the Allee threshold in finite time, but the second inequality in (5.31) requires that the population remain above a positive threshold in the wake of the invasion front for all times. This difficulty is reflected in the formulation of the result below. The following theorem summarizes several aspects of the first published work on spreading speeds and traveling waves in IDEs with Allee effect growth function.

Theorem 6.2 (Lui 1983) *Consider the IDE* $N_{t+1}(x) = (K * F(N_t))(x)$ *where*

(i) K *is a continuous, symmetric probability distribution with finite moment-generating function;*
(ii) there is a constant C *such that* $\int_x^{\infty} K(y)\mathrm{d}y \leq CK(x)$ *for large* x;
(iii) F *is continuously differentiable with* $F(0) = 0 = F(1) - 1$, *and (A1) holds;*
(iv) $F'(N) \leq F'(N_a)$ *for* $N \in [0, 1]$; *and*
(v) $F'(0)N \leq F(N) \leq F'(1)(N - 1) + 1$ *for* $N \in [0, 1]$.

Then the following statements hold.

1. *There exists an asymptotic spreading speed, c^*, in the following sense. If $N_0(x) = 0$ for $x > 0$ and $N_0(x) > N_a$ as $x \to -\infty$, then*

$$\limsup_{t\to\infty} \max_{x>(c^*+\epsilon)t} N_t(x) = 0 \quad \text{and} \quad \liminf_{t\to\infty} \min_{x<(c^*-\epsilon)t} N_t(x) = 1 \,.$$

2. *A monotone traveling wave can exist for at most one speed.*
3. *There exists $c^* \in \mathbb{R}$ and a family of monotone traveling waves with speed c^*.*

Lui's results are more general than we have stated here. The dispersal kernel can have some discontinuities, and it does not have to be symmetric. When the kernel is not symmetric, we obtain a spreading speed in each direction. The results are not more difficult to prove, but they are more tedious to state. We consider a particular form of asymmetry in Sect. 12.2. The condition on the moment-generating function may be relaxed as in the previous chapter, but some boundedness condition is necessary. When the kernel is heavy tailed, accelerating fronts do exist even with Allee effects (Wang et al. 2002, 2013).

Condition (*v*) requires the graph of F to be bounded between the tangent line at zero and the tangent line at one. Condition (*iv*) requires the slope of the growth function to be maximal at the Allee threshold. These conditions can be weakened (Pan and Zhang 2011). The two asymptotic requirements on the initial condition make it look "wave-like." Lui's original formulation is for compactly supported initial data and needs additional assumptions.

While there is no explicit formula for the speed in the presence of an Allee effect, Lui (1983) gives an upper bound of c^* as

$$c^* \le \max_{s>0} \frac{1}{s} \ln\left(\max_{N>0} \frac{F(N)}{N} M(s)\right). \tag{6.30}$$

This bound can be obtained by bounding the growth function F with a function that is monotone and concave down. Lui constructs such a function as

$$F^+(N) = \begin{cases} mN, & 0 \le N \le \tilde{N}, \\ 1, & N > \tilde{N}, \end{cases} \tag{6.31}$$

where $m = \max_{N>0} \frac{F(N)}{N}$ and $\tilde{N} = 1/m$ (Fig. 6.5, left panel). At the point $N = 1/m$ where F^+ is not differentiable, it can be "smoothed out" so that it still has the required properties. Alternatively, if F is monotone and concave down whenever it is above the diagonal, we can define F^+ as above for $N < \tilde{N}$ and $F^+ = F$ for $N \ge \tilde{N}$ (Fig. 6.5, right panel). In the latter case, the function is continuously differentiable. In both cases, F^+ is monotone and concave down. Hence, the spreading speed for the IDE with F^+ is linearly determined and given explicitly by the formula in (5.17), which becomes (6.30) for this example. Since $F \le F^+$, the spreading speed with function F is bounded above by the spreading

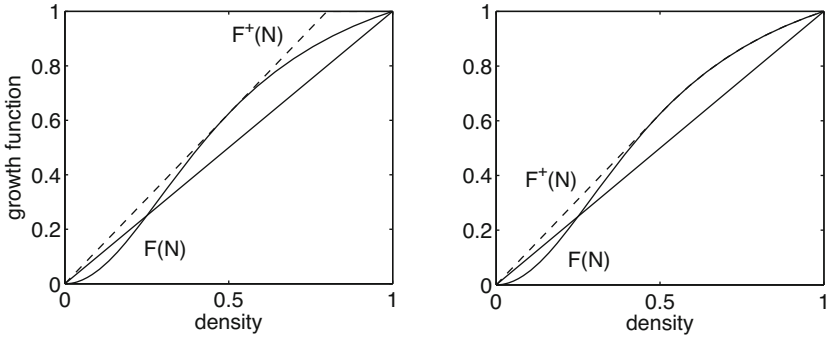

Fig. 6.5 Illustration of a function without Allee effect (F^+) bounding a function with Allee effect (F). The left panel shows the construction by Lui (1983), which has a corner. The right panel shows the alternative construction, which is smooth (see text).

speed with function F^+, as in Sect. 5.4. For the Allee function in (2.22) with $R > \gamma = 2$, we can explicitly calculate

$$m = \frac{R}{2\sqrt{R-1}} \qquad \text{and} \qquad \tilde{N} = \frac{1}{\sqrt{R-1}} \, .$$

An upper bound for the spreading speed is then given by

$$c^* \leq \max_{s>0} \frac{1}{s} \ln \left(\frac{R}{2\sqrt{R-1}} M(s) \right) \, . \tag{6.32}$$

To end this chapter, we relate the results about spreading speed to the observations about the existence of a positive steady state on a bounded domain from Sect. 4.5. There, we found that for a positive steady state to exist, we need more than just the existence of a stable positive state in the nonspatial model and a small variance of the dispersal kernel. In fact, the condition we found was independent of the variance of the dispersal kernel: it required the growth to be "strong enough." The threshold between existence and nonexistence of a positive steady state was given by $H(1) - 1/2 = H(0)$, where $H(N)$ is an antiderivative of F. For population spread with an Allee effect, formula (6.17) states that a traveling front invades only if

$$0 < \int_0^1 [F(N) - N] dN = H(1) - H(0) - 1/2 \, . \tag{6.33}$$

In other words, a steady state on a bounded domain can only exist if the speed of a traveling wave on the unbounded domain is positive. Numerically, we can observe that a locally introduced population on a bounded domain can spread in a front-like fashion to fill the domain and establish a positive steady state.

6.5 Further Reading

A comprehensive review of models for spatial spread with Allee effect can be found in Taylor and Hastings (2005) and more recent results in relation to biological invasions in Lewis et al. (2016). However, while there are many theoretical results, there are relatively few applications of the IDE with Allee effect to real ecosystems. We discuss some in Sect. 12.6.

Since the dynamics with strong Allee effect have two stable steady states, the equation is sometimes called the bistable equation. In contrast, dynamics of Beverton–Holt type have a single stable steady state and are called monostable. Accordingly, traveling fronts are sometimes called bistable fronts and monostable fronts, respectively. When the speed of a front is determined by the linearization at zero (monostable equations; see previous chapter), the front is referred to as a pulled front since the few individuals ahead of the front "pull" it along. In contrast, in the bistable equation, there has to be sufficient growth at higher density (see Theorem 6.1) to "push" the population forward. We sometimes speak of pushed fronts in that case. Bistable traveling fronts in reaction–diffusion equations have received considerably more attention than in IDEs, particularly in combustion problems. Early references can be found in Lui (1983); for recent results and extensions, see, e.g., Hamel (2016).

The original results by Lui (1983) were extended to multiple space dimensions by Creegan and Lui (1984). Later, Lui (1985) showed that solutions with compact initial data converge to a double-front profile. He also proved that solutions were trapped by translations of the traveling front. The existence and stability of clines, i.e., traveling fronts with speed zero, was shown in Lui (1986). More recently, Pan and Zhang (2011) showed the existence, uniqueness, and asymptotic stability of bistable traveling fronts for IDEs by a squeezing technique. Even more general results that include, e.g., spatially heterogeneous environments can be found in Fang and Zhao (2015). Similar, but independent results can be found in Coutinho and Fernandez (2004).

The theory for the monostable equation from Chap. 5 can be applied to prove the existence of a different kind of traveling waves in the bistable equation (Corollary after Proposition 3 in Lui 1983). We assume that F satisfies the conditions from Theorem 6.2. We define the function

$$G(N) = F(N + N_a) - N_a \,, \qquad N \in [0, 1 - N_a] \,, \tag{6.34}$$

and the IDE $N_{t+1}(x) = (K * G(N_t))(x)$. Then $G(0) = 0 = G(1 - N_a) - N_a$, $G'(0) = F'(N_a) > 1$ and $G(N) \leq G'(0)N$ on $[0, 1 - N_a]$. In other words, the IDE with growth function G satisfies all the conditions for the theory in Chap. 5. Hence, the bistable equation has monotone traveling waves that connect N_a with one, and their minimal speed is given by the formula in (5.17) with $R = G'(0)$. In Sect. 11.4, we will use the idea behind the construction of G to investigate spreading phenomena in the Ricker equation when the positive steady state is unstable.